Carrier transport properties in single-walled carbon nanotubes studied by photoluminescence spectroscopy

Y Ohno[1,2], T Shimada[3], S Kishimoto[1], S Maruyama[3] and T Mizutani[1]

[1]Department of Quantum Engineering, Nagoya University, Furo-cho, Chikusa-ku, Nagoya 464-8603, Japan
[2]PRESTO/ Japan Science and Technology Agency, 4-1-8 Honcho Kawaguchi, Saitama 332-0012, Japan
[3]Depratment of Mechanical Engineering, The University of Tokyo, 7-3-1 Hongo, Bunkyo-ku, Tokyo 133-8656, Japan

E-mail: yohno@nuee.nagoya-u.ac.jp

Abstract. We have investigated the photoluminescence (PL) of in individual single-walled carbon nanotubes (SWNTs) placed in field-effect transistor structures to study carrier transport in the SWNT. The relation between the recombination lifetime and carrier transit time has been evaluated from the drain-field dependence of PL intensity. Time-resolved photoluminescence of SWNTs dispersed in surfactant solution has also been studied to evaluate the recombination lifetime. From these results, the carrier saturation velocity was estimated.

1. Introduction

Single-walled carbon nanotubes (SWNTs) are attractive nano-scale materials for electronic and optoelectronic devices because they have a high electron mobility, high current capacity, and the energy band structures with direct transitions [1,2]. Field-effect transistors (FETs) [2], light-emitting diodes [3], and photosensitive devices [4-6] using SWNTs have already been reported. For such device applications, it is important to understand the optical and carrier transport properties of SWNTs. Photoluminescence (PL) spectroscopy is one of the most powerful techniques available for characterizing the electronic properties of SWNTs [7,8].

In this paper, we report on carrier transport properties in SWNTs studied by means of microscopic PL spectroscopy of single SWNTs placed in FET structures. Time-resolved PL spectroscopy of surfactant-wrapped SWNTs has also been investigated in order to understand the recombination mechanism of photoexcited carriers.

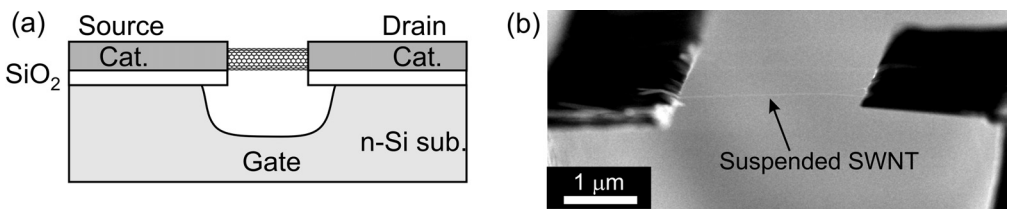

Figure 1. (a) Schematic device structure and (b) SEM image of the fabricated device.

2. Experiments

The schematic structure and an SEM image of a fabricated FET are shown in figure 1 [9]. In order to obtain sufficient luminescence from an individual SWNT, we employed a sample structure with SWNTs suspended from a substrate [10]. The device fabrication process is as follows. First, a groove with a width of ~2.5 μm was formed on a *n*-Si substrate with a 100-nm-thick SiO_2. The metal catalysts for growth of SWNTs, Co/Pt (2/10 nm) [11], were placed on both sides of the groove. The metal catalysts were also used as the S/D electrodes. The SWNTs were synthesized by chemical vapor deposition (CVD) using ethanol (100 sccm) at 800°C for 10 min. During this CVD process, SWNTs bridged between the S/D electrodes over the groove as shown in the SEM image.

Micro-PL spectroscopy was performed using an objective lens (×100), a continuous-wave Ti/Sapphire laser, a 25-cm monochromator, and a nitrogen-cooled InGaAs photomultiplier. The power and diameter of the incident laser beam on the device surface were ~20 μW and 1~2 μm, respectively. The measurements were performed in air at room temperature. In our experiments, strong PL with the spectral width of 5~15 meV was obtained from the suspended part of a SWNT, whereas no detectable signal was observed from the part lying on the SiO_2/Si substrate.

3. Effect of bias voltage

The effect of the drain bias on the PL spectrum of an individual SWNT is shown in figure 2(a). Here, V_{DS} = -0.5, 0, 0.5 V, respectively. The profile of the spectrum did not change with small V_{DS} except in intensity. When a drain bias is applied to the device, carriers excited by the incident laser might be accelerated by the field and become hot. However, neither the spectral broadening nor the change in the spectral tail on the high-energy side, which reflects the carrier temperature, were observed in the present case. Freitag *et al*. reported broad electroluminescence originating from hot carriers under high drain field [12]. In our experiment, since the drain field at ~2 kV/cm is relatively low, the electrons and holes accelerated by the drain field might immediately relax their energy and are cooled down to the conduction and valence band edges, E_C and E_V, respectively.

With increasing $|V_{DS}|$, the PL intensity monotonically decreased as shown in figure 2(b). The upper horizontal axis is the electric field (F) given by $F = V_{DS}/l$. This can be explained by the extraction of the photoexcited carriers due to the drain field as shown in the inset. In this situation, the PL intensity is determined by the relation between the recombination lifetime (τ_r) and transit time of the photoexcited carriers to the electrodes (τ_t). When V_{DS} is ~0 V and τ_t is much longer than τ_r, photoexcited carriers reside in the SWNT and recombine with emitting photons. On the other hand, when a fairly large V_{DS} is applied to the device, τ_t becomes smaller than τ_r, so that the carriers are swept out of the SWNT before the onset of radiative recombination. Consequently, PL intensity decreases with applying V_{DS}.

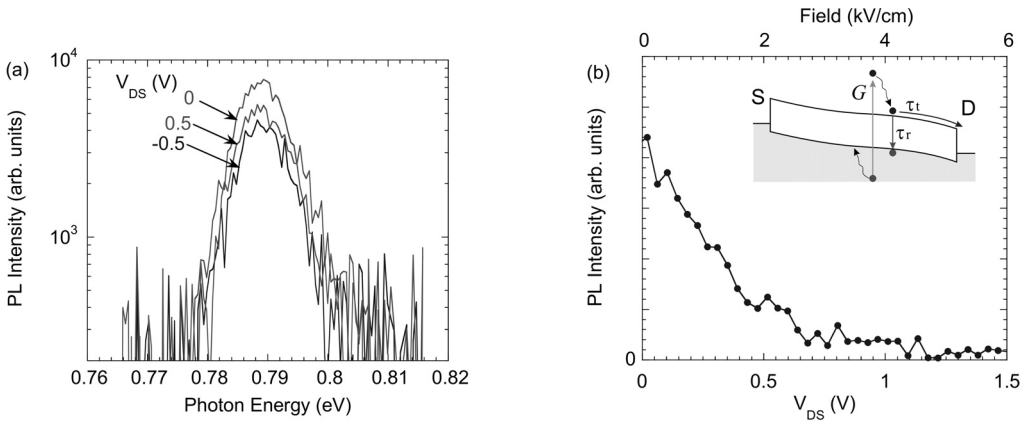

Figure 2. (a) PL spectra of a SWNT at various V_{DS} from -0.5 to 0.5 V. (b) V_{DS} dependence of PL intensity. The inset shows the band diagram and carrier behaviour in the device.

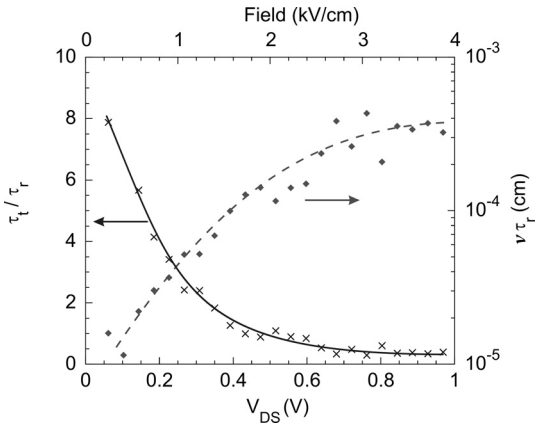

Figure 3. τ_t/τ_r and $v\tau_r$ as a function of V_{DS}.

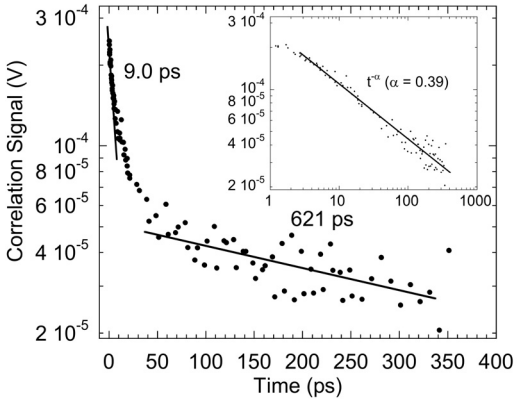

Figure 4. Time-domain correlation signal. The inset contains the log-log plot.

By solving simple rate equations for electron and hole concentrations (n and p) in the SWNT, which take into account the photoexcitation, recombination, and extraction to electrodes, PL intensity is given as a function of τ_t as follows,

$$I_{PL} \propto pn = \left(1 + \frac{\tau_r}{\tau_t}\right)^{-2} I_{PL}(0). \qquad (1)$$

Here, $I_{PL}(0)$ is the PL intensity at V_{DS} = 0 V. The effect of the drain field on the PL intensity is included in τ_t, which is determined by the field-dependent carrier velocity ($v = l/2\tau_t$). The τ_t/τ_r is evaluated from the result of figure 2(b) and eq. (1) as a function of V_{DS}, as shown by the crosses in figure 3. When F increased to ~1.5 kV/cm, the carrier transit time became equal to the recombination lifetime. The product of the carrier velocity and the recombination lifetime $v\tau_r$ is also shown in figure 3. The $v\tau_r$ increased from 1×10^{-5} to 4×10^{-4} cm with increasing F from 0.2 to 1 kV/cm, and showed a tendency to saturate at 4×10^{-4} cm. This saturation may be attributed to the carrier velocity saturation due to optical phonon scattering [13,14].

4. Time-resolved PL spectroscopy

In order to estimate the carrier velocity, we have investigated the recombination lifetime via time-resolved PL spectroscopy. The excitation correlation technique [15] was employed for the time-resolved PL measurements. The laser pulses from an optical parametric amplifier (~1 ps, 1 kHz, ~20 μJ) are divided into two separate pulse trains which are delayed in time with respect to each other and are chopped separately at two different frequencies, f_1 = 24 Hz and f_2 = 38 Hz. The PL signal at frequency difference, f_1-f_2 = 14 Hz, is detected by a liquid-N_2-cooled InGaAs photomultiplier tube and a lock-in amplifier. The resolution of this measurement is limited only by the laser pulse width. The materials used in this experiment were HiPco SWNTs dispersed in a sodiumdodecylsulfate solution.

Figure 4 shows the measured time-domain correlation signal. The excitation and detection wavelengths are 736 nm and 1056 nm, respectively, which corresponds to (10,2) SWNTs. The decay of the correlation signal cannot be expressed by a single exponential function, but seems to contain various decay times from 9.0 to 621 ps. The inset contains log-log plots of the decay signal, indicating the decay can be expressed by a power law with an exponent of -0.39. Although we do not at present have an adequate explanation of the power law decay, there are two possible mechanisms; exciton-exciton annihilation and multi-pass decay. In case of the former process, the decay time depends on carrier concentration, thus giving the power law dependence with an exponent of -0.5 [16]. In our results, the value of the exponent was -0.39, which is larger than -0.5. In the latter process,

recombination occurs through multiple passes, primarily via non-radiative recombination centers. In the excitation-intensity correlation technique, the time-domain signal generally gives the cross correlation of the populations of the levels involved in the decay process of photoexcited carriers rather than the true transient decay of the PL signal often measured by using streak cameras. Further study is necessary in order to understand the carrier relaxation mechanism in SWNTs.

The fast component of 9.0 ps measured in our experiment is fairly consistent with the reported relaxation times of the first excitonic state of 5~20 ps [17] and ~35 ps [18] for HiPco SWNTs and ~56 ps [18] for pulsed laser vaporization SWNTs which were measured by the pump-probe technique. Although the reported τ_r depends on the tube diameter, the synthesis method, and the environmental conditions, if we use the value of 5~50 ps for τ_r, the carrier saturation velocity is estimated to be 8×10^7~8×10^6 cm/s at 4 kV/cm. The saturation velocity and saturation field are consistent with theoretical works, which reported that the carrier velocity saturates at $3\sim5\times10^7$ cm/s due to optical phonon scattering [13,14].

5. Summary

We have investigated the effects of drain fields on the PL from individual SWNTs suspended in FET structures. The PL intensity decreased by the drain field due to the extraction of photoexcited carriers to the electrodes. The relation between the carrier transit time and recombination lifetime was evaluated. The time-resolved PL measured for SWNTs in surfactant solution by the excitation intensity correlation technique displayed a power law decay, suggesting the existence of multiple recombination passes. The carrier saturation velocity was estimated to be 8×10^7~8×10^6 cm/s at 4 kV/cm.

References

[1] Dresselhaus M S, Dresselhaus G and Avouris Ph 2001 *Carbon Nanotubes: Synthesis, Structures, Properties, and Applications* (Berlin: Springer)
[2] Avouris Ph 2004 *MRS Bulletin* **29** 403
[3] Misewich J A, Martel R, Avouris P, Tsang J C, Heinze S and Tersoff J 2003 *Science* **300** 783
[4] Freitag M, Martin Y, Misewich J A, Martel R and Avouris Ph 2003 *Nano Lett*. **3** 1067
[5] Ohno Y, Kishimoto S, Mizutani T, Okazaki T and Shinohara H 2004 *Appl. Phys. Lett.* **84** 1368
[6] Ohno Y, Kishimoto S and Mizutani T, 2005 *Jpn. J. Appl. Phys.* **44** 1592
[7] O'Connell M J, Bachilo S M, Huffman C B, Moore V C, Strano M S, Haroz E H, Rialon K L, Boul P J, Noon W H, Kittrell C, Ma J P, Hauge R H, Weisman R B and Smalley R E 2002 *Science* **297** 593
[8] Bachilo S M, Strano M S, Kittrell C, Hauge R H, Smalley R E and Weisman R B 2002 *Science* **298** 2361
[9] Ohno Y, Kishimoto and Mizutani T 2006 *Nanotechnology* **17** 549
[10] Lefebvre J, Finnie P and Homma Y 2003 *Phys. Rev. Lett.* **90** 217401
[11] Ohno Y, Iwatsuki S, Hiraoka T, Okazaki T, Kishimoto S, Maezawa K, Shinohara H, and Mizutani T 2003 *Jpn. J. Appl. Phys.* **42** 4116
[12] Freitag M, Perebeinos V, Chen J, Stein A, Tsang J C, Misewich J A, Martel R and Avouris Ph 2004 *Nano Lett.* **4** 1063
[13] Pennington G and Goldsman N 2003 *Phys. Rev. B* **68** 045426
[14] Perebeinos V, Tersoff J and Avouris Ph 2005 *Phys. Rev. Lett.* **94** 086802
[15] Johnson M B and McGill T C 1988 *J. Appl. Phys.* **63** 2077.
[16] Ma Y Z, Valkunas L, Dexheimer S L, Bachilo S M and Fleming G R 2005 *Phys. Rev. Lett.* **94** 157402
[17] Ostojic G N, Zaric S, Kono J, Strano M S, Moore V C, Hauge R H and Smalley R E 2004 *Phys. Rev. Lett.* **92** 117402
[18] Yang J P, Kappes M M, Hippler H and Unterreiner A N 2005 *Phys. Chem. Chem. Phys.* **7** 512